Maternal expression of a NANOS homolog is required for early development of the leech *Helobdella robusta*

Sara J. Agee, Deirdre C. Lyons, David A. Weisblat *

Department of Molecular and Cellular Biology, 385 LSA, University of California, Berkeley, CA 94720-3200, USA

Abstract

The gene *nanos* (*nos*) is a maternal posterior group gene required for normal development of abdominal segments and the germ line in *Drosophila*. Expression of *nos*-related genes is associated with the germ line in a broad variety of other taxa, including the leech *Helobdella robusta*, where zygotically expressed *Hro-nos* appears to be associated with primordial germ cells. The function of maternally inherited *Hro-nos* transcripts remains to be determined, however. Here, the function of maternal *Hro-nos* is examined using an antisense morpholino (MO) knockdown strategy, as confirmed by immunostaining and western blot analysis. HRO-NOS knockdown embryos exhibit abnormalities in the distribution of micromeres during cleavage. Subsequently, their germinal bands are positioned abnormally with respect to the embryonic midline and the micromere cap, epiboly fails, and the HRO-NOS knockdown embryos die. This lethality can be rescued by injection of mRNA encoding an eGFP::HRO-NOS fusion protein. HRO-NOS knockdown embryos make their normal complements of mesodermal and ectodermal teloblasts, and the progeny of these teloblasts segregate into distinct mesodermal and ectodermal layers. These results suggest that maternal *Hro-nos* is required for embryonic development. However, contrary to previous suggestions, maternal inherited *Hro-nos* does not appear necessary for ectoderm specification.

Introduction

nanos (*nos*) was first identified as a maternally inherited posterior group gene in the fruit fly *Drosophila melanogaster* (Nusslein-Volhard et al., 1987; Lehmann and Nusslein-Volhard, 1991). Most of the maternal *nos* transcripts are diffusely distributed throughout the zygote and are not translated (Bergsten and Gavis, 1999). A small fraction of the transcripts are localized and translated at the posterior pole (Gavis and Lehmann, 1994; Bergsten and Gavis, 1999; Irish et al., 1989; Forrest and Gavis, 2003), giving rise to a NOS protein gradient that participates in repressing translation of maternally inherited *hunchback* mRNA in the posterior of the embryo (Irish et al., 1989; Wreden et al., 1997). This repression is required for development of the abdominal segments (Irish et al., 1989). *nanos* is also required for normal development of the

Drosophila germ line (Kobayashi et al., 1996), where it is also thought to participate in repressing transcription (Deshpande et al., 1999, 2005) and translation (Asaoka-Taguchi et al., 1999).

Characterization of a *nos* homolog in *Schistocerca* (Lall et al., 2003) indicates that a dual function of *nos*-related genes, in germ line development and in early embryonic polarity, was ancestral to at least the insects. *nos* homolog transcripts are associated with the germ line in cnidarians (*Hydra*, Mochizuki et al., 2000; *Podocoryne*, Torras et al., 2004; *Nematostella*, Extavour et al., 2005), nematodes (Subramaniam and Seydoux, 1999; Kraemer et al., 1999), and vertebrates (*Xenopus*, Mosquera et al., 1993; MacArthur et al., 1999; zebrafish Koprunner et al., 2001; mouse, Tsuda et al., 2003), but there is no evidence for involvement of maternal *nos* homologs in patterning the early embryos in any of these taxa, with the possible exception of cnidarians. In the sea anemone *Nematostella vectensis*, one of two *nos*-class genes is present as a maternal transcript (Extavour et al., 2005) that either persists or

is selectively re-expressed in prospective endoderm during gastrulation (Extavour et al., 2005).

In the glossiphoniid leech *Helobdella robusta* (phylum Annelida), a *nanos* ortholog (*Hro-nos*) is also expressed both maternally and zygotically (Pilon and Weisblat, 1997; Kang et al., 2002). Could these observations mean that a maternally expressed *nanos*-class gene functioned in patterning the embryo of the protostome ancestor (the results from nematodes notwithstanding), or are they an example of convergent evolution? Zygotic expression of *Hro-nos* is eventually restricted to presumptive primordial germ cells (Kang et al., 2002), but the developmental significance of the maternally inherited *Hro-nos* transcripts remains to be determined. Elucidating the function of maternal *Hro-nos* should contribute to distinguishing between these possibilities.

As with other clitellate annelids, *Helobdella* oocytes are fertilized internally but arrest in metaphase I of meiosis until after zygote deposition. Between polar body formation and first cleavage, cytoplasmic rearrangements form domains of yolk-deficient cytoplasm (teloplasm) at the animal and vegetal poles of the zygote (Astrow et al., 1989; Holton et al., 1994; Fig. 1A). During cleavage, teloplasm is segregated to the D quadrant and thence to the segmentation stem cells (teloblasts) that constitute the posterior growth zone of the clitellate embryo (Weisblat and Huang, 2001; Fig. 1A). *Hro-nos* mRNA is abundant in the oocyte; its localization and translation in the early embryo have been analyzed by northern and western blots, in situ hybridization, and immunostaining on intact embryos and dissected blastomeres (Pilon and Weisblat, 1997; Kang et al., 2002).

Hro-nos transcripts become localized to the teloplasm in the zygote and are equally distributed between the animal and vegetal hemispheres (Kang et al., 2002). Transcript levels decline gradually during cleavage (Pilon and Weisblat, 1997). Translation appears to be delayed until fertilization; HRO-NOS

protein is first detected in the 2-cell stage. It should be noted that we cannot exclude the possibility that *Hro-nos* is being transcribed zygotically during cleavage. But since *Hro-nos* transcript levels are decreasing continuously from the levels present in the oocyte (Pilon and Weisblat, 1997), it is most likely that this early HRO-NOS expression represents translation primarily if not exclusively from maternal transcripts.

HRO-NOS expression peaks at fourth cleavage as macromere D′ cleaves to form proteloblasts DM and DNOPQ, precursors of segmental mesoderm and ectoderm, respectively (Fig. 1). At this stage, HRO-NOS is more highly expressed in the ectodermal precursor DNOPQ than in the mesodermal precursor DM (Pilon and Weisblat, 1997). This difference in HRO-NOS protein levels correlates with the distribution of maternal *Hro-nos* mRNA, which is also more abundant in DNOPQ than in DM (Kang et al., 2002). This could represent either differential localization or differential stabilization, or both, because the overall levels of *Hro-nos* are decaying during cleavage (Pilon and Weisblat, 1997). In the context of previous embryological studies on the specification of ectoderm in leech (Nelson and Weisblat, 1991, 1992), these observations led to the proposal that translation of maternal *Hro-nos* may function in specifying DNOPQ as ectoderm, which would represent a novel function for *nanos*-class genes (Pilon and Weisblat, 1997).

To test this hypothesis, we have examined the developmental function of maternal *Hro-nos* mRNA, using an antisense morpholino oligomer (AS MO) to knock down HRO-NOS expression. HRO-NOS knockdown embryos formed the normal complements of mesodermal and ectodermal teloblasts, contrary to the hypothesis that maternal expression of HRO-NOS is a critical factor in specifying the different fates of mesodermal (DM) and ectodermal (DNOPQ) precursors. Instead, embryos with reduced HRO-NOS expression arrested in development near the onset of epiboly. This developmental arrest was preceded by disorganization of the micromere cap during
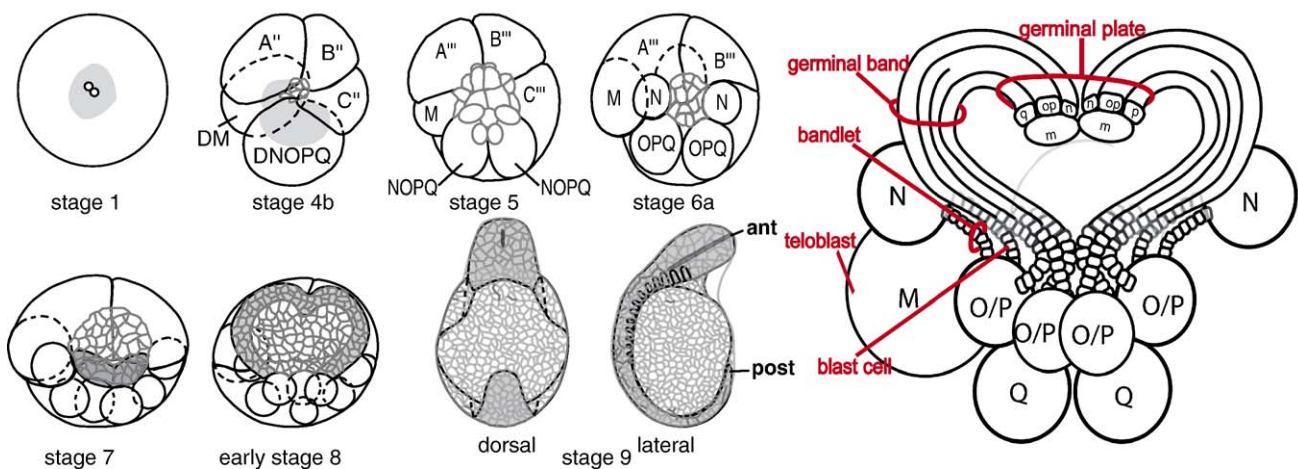

Fig. 1. Relevant stages of *H. robusta* development. Drawings depict animal pole/dorsal views (anterior up) at all stages, plus lateral views (anterior to left) of selected stages. See text for details. Polar bodies are depicted by small circles at early stage 1. Teloplasm is depicted by shading at late stages 1 and 4b. Micromeres and their derivatives are outlined in gray in stages 4b–9. Germinal bands and germinal plate are indicated by gray shading under the micromere-derived epithelium in stages 7–9. The relationship of the teloblasts and their derivatives at early stage 8 (animal/dorsal view) is shown in greater detail in the drawing at right. Abbreviations: ant, anterior; post, posterior.

cleavage and failure of the germinal bands to assume their normal positions with respect to the midline of the embryo and the micromere cap.

Materials and methods

Embryos and microinjection

Embryos were obtained from two colonies of the glossiphoniid leech *H. robusta*, one from Sacramento, CA (Shankland et al., 1992) and the other from Austin, TX (Seaver and Shankland, 2000) and cultured as described previously (Weisblat and Blair, 1984). Embryos were staged as described previously (Weisblat and Huang, 2001). Alternatively, embryonic age was expressed in terms of time after zygote deposition (AZD).

Microinjection of fluorescent lineage tracers and mRNAs was carried out as previously described (Weisblat et al., 1980; Zhang and Weisblat, 2005). mRNAs encoding nuclearly localized beta-galactosidase (nLacZ) and enhanced Green Fluorescent Protein (eGFP) were transcribed in vitro from *Not*I linearized plasmids pCS2+nLacZ and pCS2+eGFP using the SP6 mMessage Machine kit (Ambion). RNase-free microinjection needles contained 0.25 µg/µl of mRNA in RNase-free water. Injections were monitored by observing the movement of yolk particles within the cytoplasm, and we estimate that the injectant is diluted several hundred fold upon injection into the zygote. Injected embryos were cultured in HL medium supplemented with 1000 U/µl Pen–Strep (Sigma).

HRO-NOS knockdown and analysis

Morpholino oligomers (MOs; Gene-Tools, Philomath, OR) were designed to complement nucleotides −5 to +20 of *Hro-nos* (Sacramento; Fig. 2A). The exact sequences of the MO used are: AS *Hro-nos* MO (5′-CGTGAACTTGTGGAT-GACATTTTTA-3′) and MM *Hro-nos* MO (5′-CGTGtACTTcTGGATcACA-TaTTTA-3′). Stock solutions of MO (4 mM) were stored at 4°C and mixed with fast green (4% in 0.2 N KCl) at a ratio of 40:1 (MO:fast green) prior to injection.
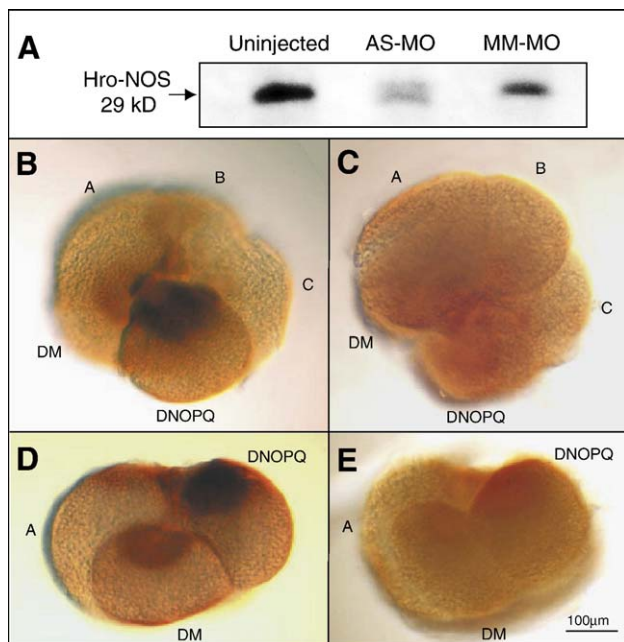

Fig. 2. AS *Hro-nos* MO knocks down HRO-NOS expression. (A) Western blot comparing the expression of HRO-NOS at stage 4b (5 embryos per lane) in uninjected embryos or after injection at early stage 1 with AS *Hro-nos* MO (AS MO) or MM *Hro-nos* MM (MM-MO). (B–E) Animal (B and C) and lateral (D and E) views of stage 4b embryos immunostained for HRO-NOS after injection at early stage 1 with either control (MM *Hro-nos* MO; B and D) or antisense (AS *Hro-nos* MO; C and E) morpholino oligomers. Scale bar, 100 µm.

Upon injection, we estimate that the MO concentration in the embryos was roughly 10 µM.

Purification of anti-HRO-NOS antibodies, immunostaining, and western blotting were carried out as described previously (Pilon and Weisblat, 1997) with minor modifications (details available upon request).

HRO-NOS rescue

To rescue the knockdown of HRO-NOS expression, the full coding region and 3′ UTR of *Hro-nos* were amplified from the stage 1 to 6 *H. robusta* cDNA library using forward primer eGNF1 and reverse primer eGNR4, designed to include *Eco*RI restriction sites and to maintain the coding region in frame (Fig. 2A), as follows: eGNF1 (gaa ttc aat gtc atc cac aag ttc acg); eGNR4 (gaa ttc gag tga atg aga tca gag g). PCR reactions included 1× Taq Gold PCR buffer II, 2.5 mM MgCl₂, 1 µM eGNF1, 1 µM eGNR4, 0.25 µM dNTP, 0.5 µl Taq Gold, and 0.5 µl of stage 1 to 6 *H. robusta* cDNA library (Stratagene) in a final volume of 20 µl. PCR was carried out in a BioRad Gradient Thermal cycler with one activation cycle at 94°C for 10 min, 35 amplification cycles (95°C for 30 s, 50°C for 30 s, 72°C for 1 min), and one final extension cycle at 72°C for 10 min. Product was run out and excised from a 1% agarose gel and purified (Gel extraction kit, Qiagen), and the fragment was cloned into pGEM-TEZ plasmid (Promega) following the manufacturer's protocol, yielding the plasmid pGTZ/Hronos/fl. To insert the full-length *Hro-nos* into the expression vector pCS2+eGFP, full-length *Hro-nos* was excised from pGTZ/Hronos/fl using *Eco*RI and purified (Gel purification kit, Qiagen). The pCS2+eGFP vector was digested with *Eco*RI, gel-purified, treated with CIP (NEB, in 1× NEBuffer 3) to reduce self-ligations, and ligated with the excised *Hro-nos* fragment, in a reaction containing a 1:4 vector insert ratio, yielding the plasmid pGFP:Hronos/fl. Expression and microinjection of *egfp::Hro-nos* mRNA from pGFP:Hronos/fl were carried out as described above.

Imaging and image processing

Live embryos were viewed initially on a dissecting scope and photographed digitally (Nikon Cool Pix). For more detailed analyses, embryos were viewed under a compound microscope (Nikon E800) using bright field, Nomarski, dark field, and fluorescent illumination. Images were captured with a CCD camera (Roper Scientific, Trenton, NJ) using Metamorph version 5.2 (Universal Instruments, Downington, PA). Stacks were processed frame by frame and montaged using Adobe Photoshop. To assess the expression of eGFP::HRO-NOS following injection of *egfp::Hro-nos* mRNA, identical settings for the microscope and CCD camera were used to capture fluorescent images of injected and control embryos. The resulting images were scaled manually in parallel to preserve differences.

Results

Injection of antisense morpholino oligomers knocks down maternal expression of HRO-NOS

To disrupt the early expression of HRO-NOS, which is presumably driven by the maternal *Hro-nos*, an antisense morpholino oligomer (AS *Hro-nos* MO) was designed to target the translation start site of *Hro-nos* mRNA. As a control for sequence specificity, an oligomer of the same composition, but with four mismatched bases (MM *Hro-nos* MO), was used.

It has been shown previously that translation of maternal *Hro-nos* begins during stage 2 (after first cleavage) and that HRO-NOS protein levels peak at stage 4b (9–13 h AZD) (Pilon and Weisblat, 1997). Thus, MOs were injected into zygotes (stage 1, 0–4 h AZD) and the resultant embryos were screened for HRO-NOS expression at stage 4b by western blot and immunostaining. Preliminary experiments suggested that earlier

injection of AS *Hro-nos* MO resulted in higher efficacy of HRO-NOS knockdown. Thus, all injections reported here were carried out before teloplasm formation (0–3 h AZD).

Western blotting was used to obtain a quantitative estimate of the HRO-NOS knockdown (Fig. 2), and the results of 6 experiments were analyzed. Embryos injected with AS *Hro-nos* MO (4 mM) had HRO-NOS levels that averaged 41% (±13% SD) of uninjected siblings, i.e., a 59% knockdown. Embryos injected with MM *Hro-nos* MO (4 mM) averaged 84% (±16% SD) of uninjected siblings, i.e., a 16% knockdown, a statistically significant difference (two-tailed paired Student's *t* test, $P < 0.0005$). The slight knockdown observed with the mismatch MO could reflect either a non-specific effect of the injection and/or interference with *Hro-nos* translation by the mismatched oligomer. Consistent with the former possibility, embryos injected with water only show a knockdown that is not significantly different from that obtained with injection of MM *Hro-nos* MO (data not shown).

Immunostaining revealed that in uninjected embryos (Pilon and Weisblat, 1997) and embryos injected with MM *Hro-nos* MO (Figs. 2B, D), HRO-NOS was expressed at higher levels in DNOPQ than in DM at stage 4b. In contrast, HRO-NOS expression could not be detected above background levels in immunostained embryos derived from zygotes injected with AS *Hro-nos* MO (Figs. 2C, E).

HRO-NOS knockdown is lethal

Visual inspection revealed that more than 95% of the embryos (52/54) injected with the AS *Hro-nos* MO in early stage 1 either died or were severely abnormal by the time control embryos had completed epiboly and germinal plate formation (stage 9; 120 h AZD); the 2 embryos that developed normally to stage 9 may be attributed to unsuccessful injections. In contrast, most (11/13) embryos injected with the control MM *Hro-nos* MO developed normally until the termination of the experiment at stage 9 (Fig. 3A). These differences were statistically significant ($P < 0.0001$; Fisher's exact 2-tailed probability test) whether the embryos were categorized as live versus dead or normal versus abnormal.

To test the possibility that AS *Hro-nos* MO exhibits non-specific toxicity, we sought to rescue the AS MO-injected embryos by injecting a synthetic, HRO-NOS-encoding mRNA whose expression would not be sensitive to the effects of AS *Hro-nos* MO. For this purpose, an *egfp::Hro-nos* fusion construct was designed. This construct contains the entire coding region and full-length 3′ UTR of *Hro-nos* plus a downstream SV40 polyadenylation site, fused to the carboxyl terminus of eGFP in the expression vector pCS2+ (see Materials and methods for details). Therefore, this construct contained no target sequence for AS *Hro-nos* MO, and its expression could be monitored in vivo by GFP fluorescence. We found that *egfp::Hro-nos* mRNA injected into early stage 1 embryos was translated, as judged by GFP fluorescence at stage 4b (Figs. 3B, C). Moreover, GFP fluorescence was highest in cell DNOPQ, as is endogenous HRO-NOS expression (Pilon and Weisblat, 1997).

Finally, to distinguish specific and non-specific effects of AS *Hro-nos* MO injection and the associated HRO-NOS knockdown, embryos were injected first with the AS *Hro-nos* MO and then with *egfp::Hro-nos* mRNA. Embryos injected with both AS *Hro-nos* MO and *egfp::Hro-nos* mRNA during early stage 1 showed a significant increase in viability compared to embryos injected with only the AS *Hro-nos* MO (Fig. 3A). These results

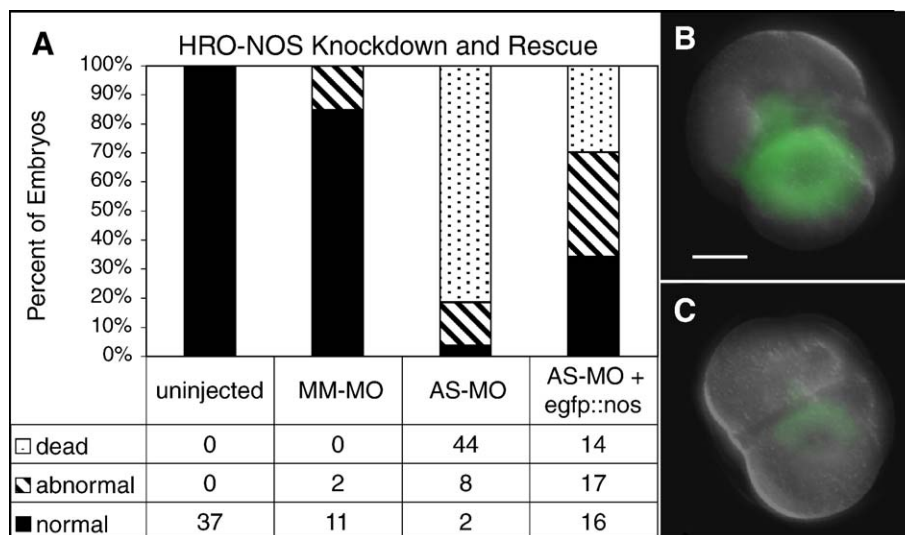| A	HRO-NOS Knockdown and Rescue			
	uninjected	MM-MO	AS-MO	AS-MO + egfp::nos
□ dead	0	0	44	14
◨ abnormal	0	2	8	17
■ normal	37	11	2	16

Fig. 3. HRO-NOS knockdown is lethal and can be rescued by expression of eGFP::HRO-NOS. (A) Table showing the distribution of outcomes (scored when uninjected controls had reached stage 9) for embryos arising from zygotes injected at early stage 1 with MM *Hro-nos* MO (MM MO), AS *Hro-nos* MO (AS MO) or AS MO followed by a second injection of *egfp::Hro-nos* mRNA. Note that even injection of MM MO control resulted in some abnormal embryos, presumably due to experimental trauma, and yet a substantial proportion of AS MO-injected embryos were partially or completely rescued by a second injection of *egfp::Hro-nos* mRNA. (B) Combined GFP epifluorescence (green) and brightfield images of a representative living stage 4b embryo arising from a zygote injected with *egfp::Hro-nos*. The distribution of eGFP::HRO-NOS resembles that of native HRO-NOS (compare with Figs. 2B, C). Similarly scaled and processed images of an uninjected control embryo to show the autofluorescence at the GFP wavelength. Scale bar, 100 μm.

support the conclusion that the lethality induced by early stage 1 injections of AS *Hro-nos* MO results from the specific knockdown of HRO-NOS expression. A corollary of this result is that the eGFP::HRO-NOS fusion protein provides functional HRO-NOS activity.

HRO-NOS knockdown does not convert ectoderm to mesoderm

Despite the fact that they were to die later, embryos in which HRO-NOS had been knocked down with AS *Hro-nos* MO appeared normal at stage 4b (11 h AZD), when mesodermal and ectodermal proteloblasts (DM and DNOPQ, respectively) were born (Fig. 4). Moreover, the subsequent cleavage divisions leading to teloblast formation also proceeded in parallel between AS *Hro-nos* MO-injected and control (MM *Hro-nos* MO-injected and uninjected) embryos, so that one pair of larger, presumptive mesoteloblasts arose from cell DM and 4 pairs of smaller, presumptive ectoteloblasts arose from cell DNOPQ by the time control embryos had reached stage 7 (Fig. 4). By these criteria, therefore, and contrary to our previous hypothesis, it appeared that a partial knockdown of maternal HRO-NOS expression did *not* convert the ectodermal proteloblast to a mesodermal fate.

HRO-NOS knockdown disrupts germinal band position

To further characterize the HRO-NOS knockdown morphotype in *Helobdella*, we first used cell lineage tracing to examine features of the lineages leading to segmental mesoderm and ectoderm. For this purpose, proteloblasts DM (stage 4; 9–12 h AZD) or OPQ (stage 6a; 18 h AZD) or teloblast N (stage 6a) were injected with mRNA encoding a nuclearly localized beta-galactosidase (nLacZ) as a lineage tracer (Zhang and Weisblat, 2005). The tracer-labeled embryos were fixed and stained for beta-galactosidase activity when controls were at early stage 8 (~72 h AZD in TX).

At early stage 8 in control embryos (both uninjected and those injected with MM *Hro-nos* MO), bandlets of primary blast cells extend from the various teloblasts to where they enter the posterior ends of the germinal bands at the surface of the embryo (Fig. 1). Each germinal band at this stage is roughly semi-circular in shape. Together, the left and right germinal bands surround a group of micromere-derived cells in prospective dorsal territory (Figs. 1, 5A–C). The germinal bands and the dorsal territory between them are covered by an epibolizing, micromere-derived epithelium (Smith and Weisblat, 1994). In normal development, the germinal bands undergo epibolic movements over the surface of the macromeres beneath the leading edge of the micromere-derived epithelium, coalescing gradually into the germinal plate, from which definitive segments arise (Fig. 1). In contrast to the controls, the germinal bands in HRO-NOS knockdown embryos lay roughly parallel to one another next to the dorsal midline. The germinal bands were markedly shorter than those in control embryos and never underwent epibolic movements. This perturbation was seen when either mesodermal or ectodermal bandlets were labeled (Figs. 5D–F) and is never seen in normal development.

Within each germinal band, the mesodermal (m) bandlets normally lie atop the yolky macromeres, and the 4 ectodermal bandlets (n, o, p, and q) are arranged over the m bandlet in contact with the micromere-derived epithelium (Fig. 1). Another feature of the ectodermal lineages is that the OP proteloblast generates four op blast cells and then divides
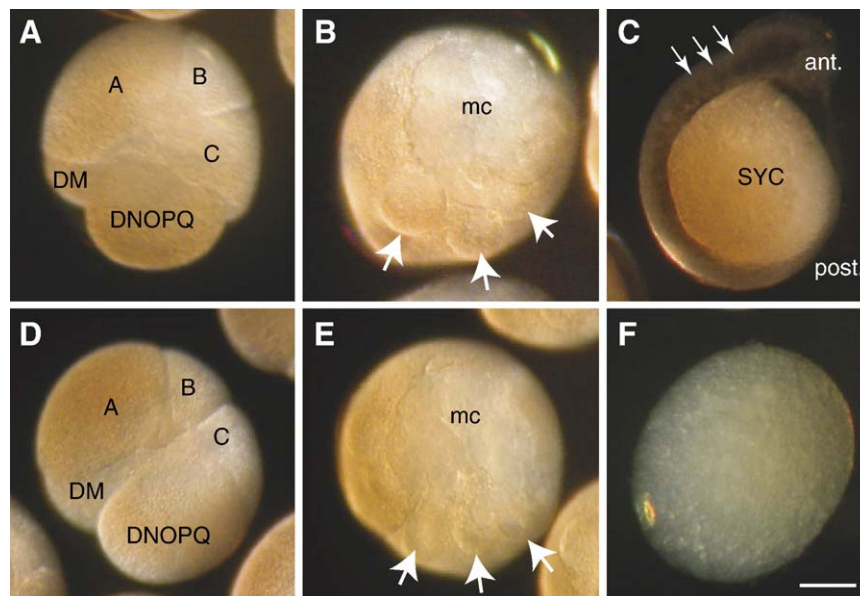

Fig. 4. HRO-NOS knockdown embryos cleave normally, yet die by stage 9. Micrographs taken when controls were at stage 4 (A, D) stage 7 (B, E) and stage 9 (C, F) of embryos arising from zygotes injected with MM *Hro-nos* MO (A–C) or AS *Hro-nos* MO (D–F). These embryos typically cleaved normally through stage 4 (macromeres and proteloblasts are labeled in panels A and C), and by stage 7 had formed a distinct micromere cap and a normal complement of teloblasts (3 of which are indicated by arrows in panels B and E). But by the time control embryos had reached stage 9 (C, arrows indicate segmental coelomic cavities), many AS *Hro-nos* MO-injected embryos were dead (F). Abbreviations: ant, anterior; mc, micromere cap; post, posterior; SYC, syncytial yolk cell. Scale bar, 100 μm.
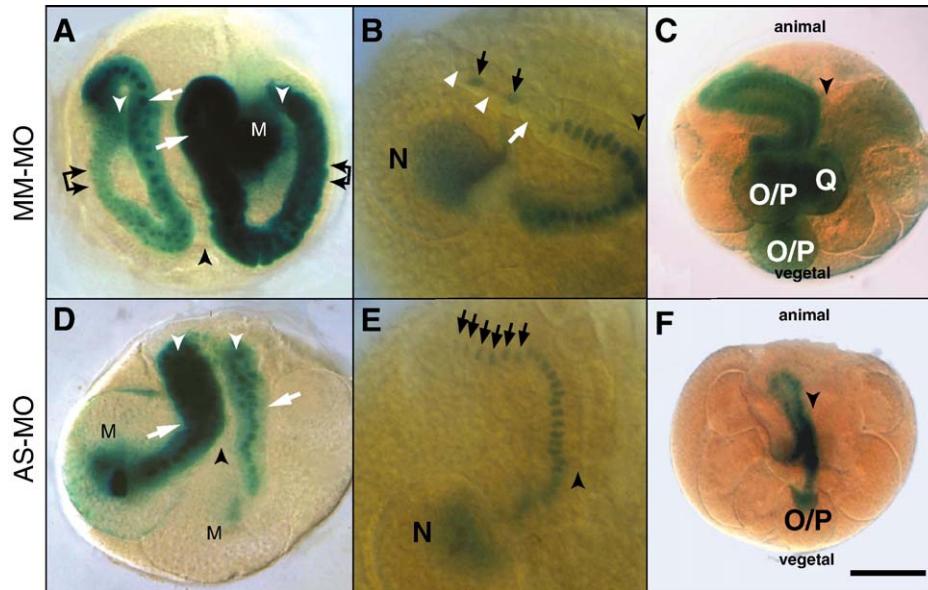
Fig. 5. HRO-NOS knockdown disrupts the positioning of germinal bands with respect to the midline. Photomontaged images combining the in focus portions of optical sections extending part way through embryos arising from zygotes injected with MM *Hro-nos* MO (MM MO; A–C) or AS *Hro-nos* MO (AS MO; D–F). Blastomeres were injected with *nLacZ* mRNA at selected points during cleavage, and the resultant embryos were fixed and processed histochemically to visualize beta-galactosidase activity (blue) at ~72 h AZD (corresponding to early stage 8 in normal development). In each panel, the point at which the bandlets reach the surface of the embryo and enter the germinal band is indicated (vertically oriented black arrowhead). When the DM″ proteloblast was injected with *nLacZ* mRNA, two mesoteloblasts (M) and their descendant bandlets are labeled in both control (A) and HRO-NOS knockdown embryos (D), but due to unequal inheritance of the injected mRNA, the left and right sides are not always equally labeled. Only one M teloblast is visible in the control embryo (A), but the two labeled m bandlets emerge from the teloblasts beneath the surface of the embryo and extend to the surface parallel to the midline. There, they merge with the (unlabeled) ectodermal bandlets to form the germinal bands. On each side, the germinal band curves out around the micromere cap, as indicated by the joined arrowheads. The point at which m blast cells undergo their first mitosis is indicated (white arrows), as are the distalmost ends of the bandlets that are visible in this image (white arrowheads). In the HRO-NOS knockdown embryo by contrast, the labeled bandlets are shorter overall and remain closely apposed even after they have reached the surface (compare the separation between vertical white arrowheads in panels A and D). The point of first m blast cell mitosis and distal ends of the bandlets are indicated as in panel A. When an N teloblast was injected, both control (B) and knockdown embryos (E) contained a single labeled bandlet, as expected. Control embryos evidenced the normal alternation of nf and ns blast cell fates; the earliest mitosis of an nf primary blast cell (marked by the loss of nuclear nLacZ activity) is seen ~24 cells distal to the teloblast (white arrow), and in the 2nd and 4th cells distal to that one (white arrowheads), while the intervening ns cells (black arrows) have not yet divided. In knockdown embryos, none of the corresponding blast cells has divided (black arrows). OPQ proteloblasts in both control (C) and knockdown embryos (F) gave rise to 3 teloblasts and bandlets. In panel C, both OPQ cells were injected, but the right germinal band is only faintly labeled, and in panel F, only two of the labeled bandlets are visible. Again, in the HRO-NOS knockdown embryos, the labeled bandlets failed to assume their normal, arched forms at the surface of the embryo. Instead, they remained near the midline of the embryo and elongated along the A/V axis. Scale bar, 100 μm for panels A, C, D, and F; 50 μm for panels B and E.

equally to generate the separate O/P teloblasts. As a result, there is a branching pattern within the germinal band where the (anterior) op bandlet gives way to separate (posterior) o and p bandlets (Bissen and Weisblat, 1987; Kuo and Shankland, 2004). The normal arrangement of bandlets within the germinal bands was retained in HRO-NOS knockdown embryos (Figs. 6A, B). The OP-derived bandlets also exhibited their normal, branched pattern in the HRO-NOS knockdown embryos (Figs. 6A, B).

One possible explanation for the shortened germinal bands would be a change in the shape of individual blast cells. Consistent with this possibility, the nLacZ-labeled blast cells in HRO-NOS did appear somewhat flattened longitudinally and broadened mediolaterally versus controls (Figs. 6C, D), but this change could not easily be expressed in quantitative terms due to the variability of blast cell shapes within the bandlets and from embryo to embryo.

Another explanation for the shortened germinal bands would be a reduction in the rate of blast cell production by teloblasts in the posterior growth zone. To investigate this possibility, rates of blast cell production for teloblast lineages were measured in control and HRO-NOS knockdown embryos. For this purpose, individual teloblasts were injected with RDA lineage tracer at various times during stages 7–8. The tracer-labeled embryos were fixed after 12 h of further development, and the number of blast cells produced during that interval was used to estimate the average rate of blast cell production. For the ectodermal lineages, no statistically significant differences were found between HRO-NOS knockdown and control embryos (not shown). But for the mesodermal lineage, a small but consistent decrease in blast cell production rates was observed in response to HRO-NOS knockdown (Fig. 6E). HRO-NOS knockdown embryos also decreased their rate of m blast cell production earlier than did controls. Using the average rates of blast cell production at the various intervals, we estimated that the total number of segmental founder cells produced by the M lineages in AS *Hro-nos* MO-injected embryos was about 16% fewer than the number produced in MM *Hro-nos* MO-injected embryos.
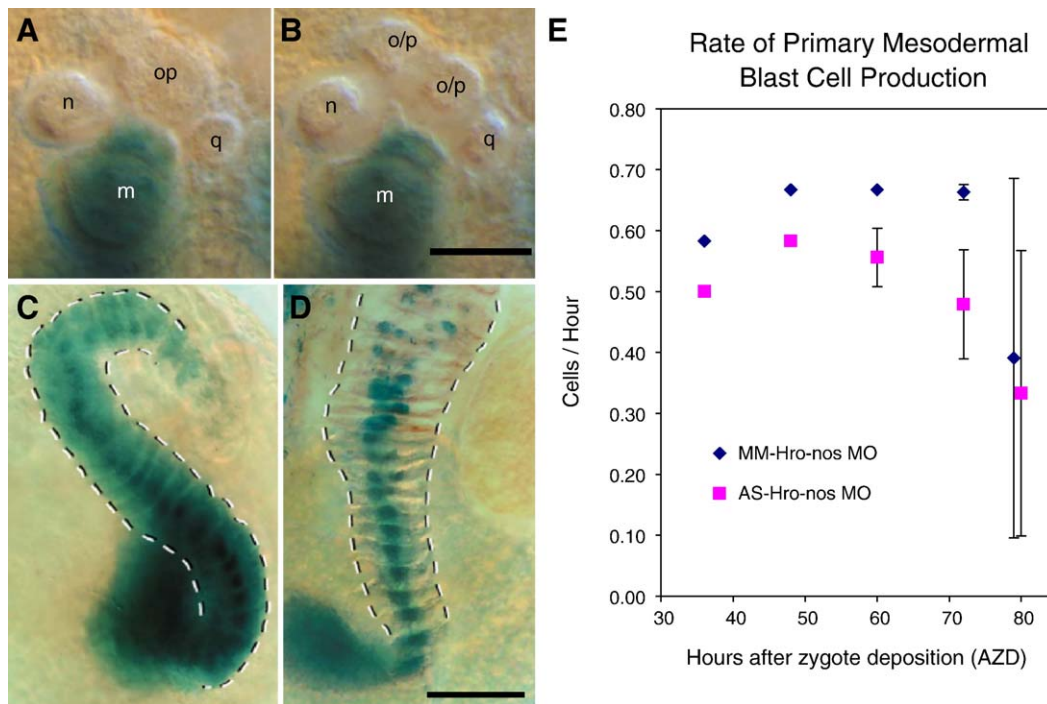
Fig. 6. HRO-NOS knockdown affects blast cell production and shape in the M lineage, but not the organization of bandlets within the germinal bands. Experimental and control embryos as described in Fig. 5. (A, B) Optical sections transverse to a germinal band in an HRO-NOS knockdown embryo in which the m bandlet was labeled with nLacZ. (A) In the anterior portion of the germinal band, 3 unlabeled bandlets lie superficial the m bandlet, corresponding to the n, op, and q bandlets produced during stage 6b, before the final cleavage of the OP proteloblasts. (B) In more posterior portions of the germinal band, 4 unlabeled bandlets are seen, as expected after the production of discrete o and p bandlets after the division of the OP proteloblast into 2 O/P teloblasts. (C, D) Dotted lines mark the edges of the m bandlets in control (C; MM Hro-nos MO-injected) and HRO-NOS knockdown (D) embryos, showing that the m bandlet becomes abnormally wide after HRO-NOS knockdown. (E) Blast cell production was measured during 12-hour intervals ending at various time points (top) in control (MM Hro-nos MO) and HRO-NOS knockdown (AS Hro-nos MO) embryos. Each point represents the average (±standard deviation) from 3 to 12 measurements. The increased variability at later time points reflects the cessation of blast cell production after the production of varying numbers of supernumerary blast cells (Desjeux and Price, 1999). Scale bar, 50 μm in panels A and B; 100 μm in panels C and D.

Division patterns of blast cells in HRO-NOS knockdown embryos

Another set of markers of bandlet identity in the *Helobdella* embryo is the timing and orientation of the mitoses of the primary blast cells within each bandlet (Zackson, 1984). Primary m blast cells divide about 10 h after they are born (i.e., when they are separated by about ~10 younger blast cells from the M teloblast). This is before the m blast cells have entered the germinal band. Moreover, the orientation of the spindle is transverse to the long axis of the bandlet so that the progeny are situated side by side within the bandlet. Primary m blast cell divisions occurred at the normal position and orientation in embryos injected with either MM *Hro-nos* MO or *Hro-nos* MO (Figs. 5A, D).

Ectodermal blast cells normally divide only after they have entered the germinal bands. They divide with their spindles oriented roughly parallel to the long axis of the bandlet, so the progeny lie roughly anterior–posterior within the bandlet. Moreover, blast cells in the n and q bandlets occur as two alternating types (nf and ns; qf and qs) which differ by several hours in cell cycle duration (Zackson, 1984; Bissen and Weisblat, 1989; Zhang and Weisblat, 2005). With the nLacZ lineage tracer, the blast cell divisions were also marked by a reduction in the intensity of the nuclear staining, reflecting dilution or degradation of the nLacZ protein upon nuclear breakdown in mitosis. This results in an alternating pattern of blast cell divisions that was readily observed in labeled n bandlets of control embryos, by virtue of the reduction in nLacZ staining in the cells that had divided (Fig. 5B). But no divisions were observed among the primary blast cells produced by the presumptive N teloblasts in HRO-NOS knockdown embryos (Fig. 5E). Thus, although the presumptive N teloblasts produced bandlets in HRO-NOS knockdown embryos, the primary blast cell divisions were either blocked or delayed beyond the time frame of our measurements.

Thus, cell lineage analysis of HRO-NOS knockdown embryos revealed that the rate of blast cell production was reduced in the mesodermal lineage, and the normal blast cell division patterns was disrupted in at least one of the ectodermal lineages. But such embryos nonetheless generated the normal complement of meso- and ectoteloblasts, and the teloblasts' progeny were positioned normally relative to one another within each germinal band. Thus, the main deficiency observed in the segmental lineages as a result of HRO-NOS knockdown was the abnormal positioning of the germinal bands with respect to the midline of the embryo.

Abnormal organization of micromere cap in HRO-NOS knockdown embryos

Previous studies have shown that ablation of specific micromeres disrupts the normal positioning and gastrulation movements of the germinal bands (Smith, 1994; Isaken, 1997), and HRO-NOS is expressed in micromeres as well as proteloblasts (Pilon and Weisblat, 1997). Could the abnormalities in germinal band positioning and the failure of epiboly in HRO-NOS knockdown embryos arise indirectly from earlier abnormalities in the micromere lineages? To investigate this possibility, we compared the distributions of micromeres within the nascent micromere cap in control and AS *Hro-nos* MO-injected embryos. For this purpose, zygotes were injected with AS *Hro-nos* MO then fixed and stained with Hoechst 33258 for comparison with control embryos at the start of stage 6 or at early stage 7 (18 or 48 h AZD, respectively).

In control (MM *Hro-nos* MO-injected) embryos fixed at the transition from stage 5 to stage 6, the micromeres were compactly arranged and occupied distinct positions (Figs. 7A–C). Descendants of the primary quartet of micromeres were still arranged in a rosette (Fig. 7B), and the nopq′ and nopq″ micromeres lay near a line between the nuclei of the nascent OPQ proteloblasts (Fig. 7C). In contrast, the micromere cap in AS *Hro-nos* MO-injected embryos was significantly wider than in controls (Fig. 7D) and the primary quartet descendants did

not form a clear rosette (Fig. 7E). In addition, the space between the nascent OPQ proteloblasts that would normally be occupied by nopq′ and nopq″ micromeres was vacant (Fig. 7F).

By early stage 7, the newly formed germinal bands in control embryos exhibited clear bilateral symmetry. The left and right germinal bands lay in a characteristic "V" orientation with their anterior ends flanking the micromere cap (Figs. 8A, C). In HRO-NOS knockdown embryos, the germinal bands were still bilaterally symmetric but formed an inverted "V" compared to controls (Figs. 8B, D). Their anterior ends butted up against the micromere cap and unlike the controls showed no indication of flanking the cap. The area of the embryo covered by the micromere cap at this stage was also reduced in HRO-NOS knockdown embryos relative to that in controls (Figs. 8B, D). Thus, the spatial relationship between the micromere cap and the nascent germinal bands was clearly abnormal at early stage 7 in HRO-NOS knockdown embryos, and this was presaged by abnormalities in micromeres themselves well before most teloblasts had even formed.

Discussion

Evolutionary ancestry of maternal expression of nos homologs

Although *nanos* (*nos*) was first identified as a segmentation gene in *Drosophila* (Nusslein-Volhard et al., 1987; Lehmann
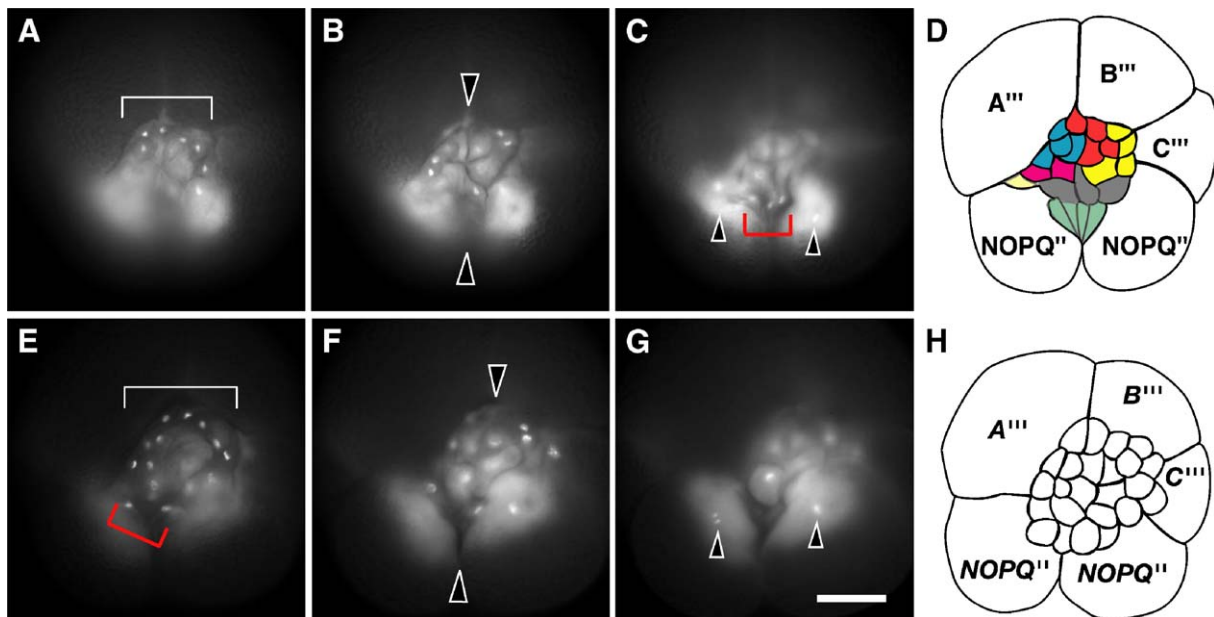

Fig. 7. HRO-NOS knockdown affects micromere organization prior to germinal band formation. Optical sections (DAPI fluorescence) through the micromere cap at progressively more vegetal levels in representative control (A–C) and HRO-NOS knockdown embryos (E–G) fixed and stained with DAPI at the start of stage 6 (defined by the initiation of cytokinesis in the NOPQ″ blastomeres; mitotic nuclei indicated by arrowheads in panels C and G). At this stage, the micromere cap in knockdown embryos (injected as zygotes with AS *Hro-nos* MO) is wider than controls (injected with MM *Hro-nos* MO; compare white brackets in panels A and E). The micromere cap in this embryo is also off center with respect to the embryonic midline as defined by the ectodermal proteloblasts (compare the arrowheads in panels B and F). Finally, the NOPQ-derived micromeres, which normally lie vegetally, near the axis connecting the proteloblast nuclei (arrowheads in panels C and G), lie closer to the animal pole in knockdown embryos (compare red brackets in panels C and E). Drawings in panels D and H show reconstructed overlays of the images shown in panels A–C and E–G, respectively. In panel D, large blastomeres are labeled and micromeres are color-coded according to their origins (Huang et al., 2002) as follows: turquoise = a‴, a″, and the 2 progeny of a′; orange = b‴, b″, and the 2 progeny of b′; dark yellow = c‴, c″, and the 2 progeny of c′; gray = dnopq′, dnopq″, and dnopq‴; green = 2 nopq′ and 2 nopq″; pink = the 2 progeny of d′; light yellow = dm′ (dm″ is not visible). In panel G, abnormal development precludes identifying the micromeres reliably; the large cells are labeled according to their nominal identities. Scale bar, 100 μm.
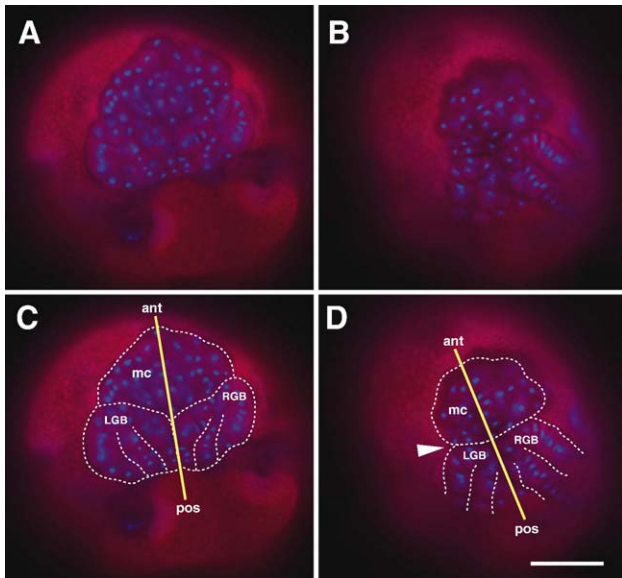
Fig. 8. HRO-NOS knockdown affects the relationship between the micromere cap and the nascent germinal bands. Combined fluorescence (DAPI) and brightfield images showing the micromere cap and nascent germinal bands in representative control (A, labeled in panel C) and HRO-NOS knockdown embryos (B, labeled in panel D), fixed at early stage 7. In control embryos, the germinal bands form a broad "V" flanking the posterior edge of the micromere cap. In HRO-NOS knockdown embryos, by contrast, the germinal bands form an inverted "V", and there is a notch (arrowhead) between the germinal bands and the micromere cap. By this point, moreover, the micromere cap is now reduced relative to controls. Abbreviations: ant, anterior; LGB, left germinal band; mc, micromere cap; pos, posterior; RGB, right germinal band. Scale bar, 100 μm.

and Nusslein-Volhard, 1991) expression of *nos*-related genes is associated with, or required for, germ line development in vertebrates (*Xenopus*, Mosquera et al., 1993; MacArthur et al., 1999; zebrafish Koprunner et al., 2001; mouse, Tsuda et al., 2003), insects (Kobayashi et al., 1996; Forbes and Lehmann, 1998; Lall et al., 2003), nematodes (Subramaniam and Seydoux, 1999; Kraemer et al., 1999), cnidarians (*Hydra*, Mochizuki et al., 2000; *Podocoryne*, Torras et al., 2004; *Nematostella*, Extavour et al., 2005), and leeches (Kang et al., 2002). These studies have led to the conclusion that the ancestral *nos*-class gene functioned in forming or maintaining the germ line.

nos-class genes are expressed maternally in insects, but not in the nematode *C. elegans*. Comparing only these taxa, it might be inferred that the A–P patterning function and maternal expression for *nos*-class genes arose within *Ecdysozoa* at some point after the separation of the lineages leading to nematodes and arthropods. But in fact, maternal expression of *nos*-class genes is also seen in vertebrates, cnidarians, and leeches. Thus, it seems likely that the *nos*-class gene was expressed maternally in the ancestral metazoan and that this feature was lost in nematode. And in that case, we must also consider the possibilities that: (1) the ancestral *nos* homolog already functioned in patterning the early embryo and that this feature was lost in the vertebrate lineage, even though it is still expressed maternally, or that; (2) the ancestral, maternal expression was coopted to serve an A–P patterning function early in the protostome lineage and this function was lost along with maternal expression in nematodes.

Further descriptive and functional studies are required to test these possibilities. Our investigations into the function of a maternally expressed *nos* homolog in *Helobdella* are a step in this direction.

Maternal Hro-nos expression is required for Helobdella development

AS *Hro-nos* MO injections in the early zygote reliably knocked down translation of the abundant maternal *Hro-nos* transcripts by ~60% in the stage 4b embryo. This partial knockdown resulted in a consistent and reproducible morphotype, consisting of a disorganized micromere cap, abnormal germinal bands, failure to undergo epiboly, and finally death of the embryo. Injecting a control MO did not cause lethality, and the AS MO-injected embryos were rescued by expression of an eGFP::HRO-NOS fusion protein, whose transcript is not complemented by AS *Hro-nos* MO. Thus, we conclude that maternal expression of the NOS homolog is essential for normal development in *H. robusta*.

We found that mesodermal and ectodermal teloblast lineages, showing most of their normal characteristics, arise from the DM and DNOPQ blastomeres, respectively, in HRO-NOS knockdown embryos. Thus, while a complete knockdown has not been achieved, our results do *not* support our previous suggestion that HRO-NOS might function in the mesoderm–ectoderm fate choice in the D lineage at fourth cleavage.

Abnormalities in micromere derivatives are seen prior to abnormalities in germinal bands

In HRO-NOS knockdown embryos, the earliest abnormalities in segmental lineages (most prominently, the persistent apposition of the germinal bands at the dorsal midline) became apparent during stages 7–8. Defects in the organization of the micromere cap were obvious as early as stage 5, which is well before the germinal bands had formed. These results are consistent with two possibilities.

One is that the primary defect resulting from HRO-NOS knockdown is within the micromere lineages and the germinal band defects are secondary. The fact that ablation of some individual micromeres disrupts the epibolic movements of the germinal bands during gastrulation (Smith, 1994; Isaken, 1997; Smith et al., 1996) suggests that such a mechanism could be operating.

A second possibility is that HRO-NOS knockdown affects both micromere (nonsegmental) and teloblast (segmental) lineages in parallel. Consistent with this alternative, HRO-NOS is expressed most prominently at stage 4b in blastomere DNOPQ, which is the precursor of all 8 ectoteloblasts and 13 of the 25 micromeres generated during cleavage in *Helobdella*.

Distinguishing between these alternatives will be complicated by the fact that origins of all 10 teloblasts and 16 of the 25 micromeres are so intertwined within the D quadrant lineage (Bissen and Weisblat, 1989). In this regard, we note that cell dnopq′ is one of the micromeres whose ablation disrupts germinal band movements, and it also expresses HRO-NOS during stage 4 (Pilon and Weisblat, 1997).

A role for nos homologs in patterning the early embryo in spiral cleavers?

Current molecular phylogenies are consistent with the "Spiralian Hypothesis", i.e., that the spiral cleavage seen in several taxa (annelids, nemerteans, molluscs, non-acoel flatworms, and echiurans) reflects their descent from a common ancestor within the proposed super-phylum Lophotrochozoa (Halanych et al., 1995). In many spiral cleavers, including leeches, the second embryonic axis is established by the segregation of determinants via asymmetric cell divisions, beginning with the first zygotic mitosis, a process referred to as "unequal cleavage". But it is generally assumed that the ancestral spiralian developed via "equal cleavage", in which each of the 4 blastomeres present after second cleavage has the potential of giving rise to the symmetry-breaking "D quadrant" (Freeman and Lundelius, 1992). For this hypothetical ancestor, as for the modern equal cleavers, a critical step in early development is the polarization that converts the fourfold symmetry of the early embryo to the bilateral symmetry of the adult.

For example, in the equally cleaving mollusc *Patella vulgata*, determination of the D quadrant results in activation of MAPK in the prospective 3D macromere at the ~32-cell stage via inductive interactions with the overlying micromeres (Lambert and Nagy, 2003). Steps upstream and downstream of the MAPK activation remain to be elucidated, but it seems clear that the micromeres can act as a signaling center in determining the second axis.

If maternal *nos* homologs were present in equally cleaving spiralians, localized translation of the maternal transcripts in a subset of the micromeres might be a symmetry-breaking event upstream of MAPK activation in the D quadrant. We speculate that this role of *nos* homologs in the micromeres might have been the ancestral condition in (equally cleaving) spiralians and that the maternal expression we see in the D quadrant proteloblasts in *Helobdella* reflects its localization to teloplasm concomitant with the evolution of unequal cleavage in clitellate annelids. Examining the expression and function of *nos* homologs in other spiral cleaving phyla should be of interest in exploring these possibilities.

Acknowledgments

References

Asaoka-Taguchi, M., Yamada, M., Nakamura, A., Hanyu, K., Kobayashi, S., 1999. Maternal Pumilio acts together with Nanos in germline development in *Drosophila* embryos. Nat. Cell Biol. 1, 431–437.

Astrow, S.H., Holton, B., Weisblat, D.A., 1989. Teloplasm formation in a leech, *Helobdella triserialis*, is a microtubule-dependent process. Dev. Biol. 135, 306–319.

Bergsten, S.E., Gavis, E.R., 1999. Role for mRNA localization in translational activation but not spatial restriction of nanos RNA. Development 126, 659–669.

Bissen, S.T., Weisblat, D.A., 1987. Early differences between alternate n blast cells in leech embryo. J. Neurobiol. 18, 251–269.

Bissen, S.T., Weisblat, D.A., 1989. The duration and compositions of cell cycles in embryos of the leech, *Helobdella triserialis*. Development 106, 105–118.

Deshpande, G., Calhoun, G., Yanowitz, J.L., Schedl, P.D., 1999. Novel functions of *nanos* in downregulating mitosis and transcription during the development of the *Drosophila* germline. Cell 99, 271–281.

Deshpande, G., Calhoun, G., Jinks, T.M., Polydorides, A.D., Schedl, P., 2005. Nanos downregulates transcription and modulates CTD phosphorylation in the soma of early *Drosophila* embryos. Mech. Dev. 122, 645–657.

Desjeux, I., Price, D.J., 1999. The production and elimination of supernumerary blast cells in the leech embryo. Dev. Genes Evol. 209, 284–293.

Extavour, C.G., Pang, K., Matus, D.Q., Martindale, M.Q., 2005. *vasa* and *nanos* expression patterns in a sea anemone and the evolution of bilaterian germ cell specification mechanisms. Evol. Dev. 7, 201–215.

Forbes, A., Lehmann, R., 1998. Nanos and Pumilio have critical roles in the development and function of *Drosophila* germline stem cells. Development 125, 679–690.

Forrest, K.M., Gavis, E.R., 2003. Live imaging of endogenous RNA reveals a diffusion and entrapment mechanism for *nanos* mRNA localization in *Drosophila*. Curr. Biol. 13, 1159–1168.

Freeman, G., Lundelius, J.W., 1992. Evolutionary implications of the mode of D quadrant specification in coelomates with spiral cleavage. J. Evol. Biol. 5, 205–247.

Gavis, E.R., Lehmann, R., 1994. Translational regulation of nanos by RNA localization. Nature 369, 315–318.

Halanych, K.M., Bacheller, J.D., Aguinaldo, A.M., Liva, S.M., Hillis, D.M., Lake, J.A., 1995. Evidence from 18S ribosomal DNA that the lophophorates are protostome animals. Science 267, 1641–1643.

Holton, B., Wedeen, C.J., Astrow, S.H., Weisblat, D.A., 1994. Localization of polyadenylated RNAs during teloplasm formation and cleavage in leech embryos. Roux's Arch. Dev. Biol. 204, 46–53.

Huang, F.Z., Kang, D., Ramierz-Weber, F.-A., Bissen, S.T., Weisblat, D.Å., 2002. Micromere lineages in the glossiphoniid leech *Helobdella robusta*. Development 129, 719–732.

Irish, V., Lehmann, R., Akam, M., 1989. The *Drosophila* posterior-group gene *nanos* functions by repressing *hunchback* activity. Nature 338, 646–648.

Isaken, D.E., 1997. The identification of a TGF-beta class gene and the regulation of endodermal precursor cell fusion in the leech. Ph.D. thesis. Dept. of Molecular and Cell Biology, University of California, Berkeley.

Kang, D., Pilon, M., Weisblat, D.A., 2002. Maternal and zygotic expression of a *nanos*-class gene in the leech *Helobdella robusta*: primordial germ cells arise from segmental mesoderm. Dev. Biol. 245, 28–41.

Kobayashi, S., Yamada, M., Asaoka, M., Kitamura, T., 1996. Essential role of the posterior morphogen *nanos* for germline development in *Drosophila*. Nature 380, 708–711.

Koprunner, M., Thisse, C., Thisse, B., Raz, E., 2001. A zebrafish *nanos*-related gene is essential for the development of primordial germ cells. Genes Dev. 15, 2877–2885.

Kraemer, B., Crittenden, S., Gallegos, M., Moulder, G., Barstead, R., Kimble, J., Wickens, M., 1999. NANOS-3 and FBF proteins physically interact to control the sperm–oocyte switch in *Caenorhabditis elegans*. Curr. Biol. 9, 1009–1018.

Kuo, D.H., Shankland, M., 2004. A distinct patterning mechanism of O and P cell fates in the development of the rostral segments of the leech *Helobdella robusta*: implications for the evolutionary dissociation of developmental pathway and morphological outcome. Development 131, 105–115.

Lall, S., Ludwig, M.Z., Patel, N.H., 2003. *Nanos* plays a conserved role in axial patterning outside of the *Diptera*. Curr. Biol. 13, 224–229.

Lambert, J.D., Nagy, L.M., 2003. The MAPK cascade in equally cleaving spiralian embryos. Dev. Biol. 263, 231–241.

Lehmann, R., Nusslein-Volhard, C., 1991. The maternal gene *nanos* has a central role in posterior pattern formation of the *Drosophila* embryo. Development 112, 679–691.

MacArthur, H., Bubunenko, M., Houston, D.W., King, M.L., 1999. *Xcat2* RNA is a translationally sequestered germ plasm component in *Xenopus*. Mech. Dev. 84, 75–88.

Mochizuki, K., Sano, H., Kobayashi, S., Nishimiya-Fujisawa, C., Fujisawa, T., 2000. Expression and evolutionary conservation of *nanos*-related genes in *Hydra*. Dev. Genes Evol. 210, 591–602.

Mosquera, L., Forristall, C., Zhou, Y., King, M.L., 1993. A mRNA localized to the vegetal cortex of *Xenopus* oocytes encodes a protein with a *nanos-like* zinc finger domain. Development 117, 377–386.

Nelson, B.H., Weisblat, D.A., 1991. Conversion of ectoderm to mesoderm by cytoplasmic extrusion in leech embryos. Science 253, 435–438.

Nelson, B.H., Weisblat, D.A., 1992. Cytoplasmic and cortical determinants interact to specify ectoderm and mesoderm in the leech embryo. Development 115, 103–115.

Nusslein-Volhard, C., Frohnhofer, H.G., Lehmann, R., 1987. Determination of anteroposterior polarity in *Drosophila*. Science 238, 1675–1681.

Pilon, M., Weisblat, D.A., 1997. A *nanos* homolog in leech. Development 124, 1771–1780.

Seaver, E.C., Shankland, M., 2000. Leech segmental repeats develop normally in the absence of signals from either anterior or posterior segments. Dev. Biol. 224, 339–353.

Shankland, M., Bissen, S.T., Weisblat, D.A., 1992. Description of the Californian leech *Helobdella robusta* sp. nov., and comparison with *Helobdella triserialis* on the basis of morphology, embryology, and experimental breeding. Can. J. Zool. 70, 1258–1263.

Smith, C.M., 1994. Developmental fats of micromeres in leech embryos and their roles in morphogenesis. Ph.D. thesis. Dept. of Molecular and Cell Biology, University of California, Berkeley.

Smith, C.M., Weisblat, D.A., 1994. Micromere fates maps in leech embryos: lineage-specific differences in rates of cell proliferation. Development 120, 3427–3438.

Smith, C.M., Lans, D., Weisblat, D.A., 1996. Cellular mechanisms of epiboly in leech embryos. Development 122, 1885–1894.

Subramaniam, K., Seydoux, G., 1999. *nos-1* and *nos-2*, two genes related to *Drosophila nanos*, regulate primordial germ cell development and survival in *Caenorhabditis elegans*. Development 126, 4861–4871.

Torras, R., Yanze, N., Schmid, V., Gonzalez-Crespo, S., 2004. *nanos* expression at the embryonic posterior pole and the medusa phase in the hydrozoan *Podocoryne carnea*. Evol. Dev. 6, 362–371.

Tsuda, M., Sasaoka, Y., Kiso, M., Abe, K., Haraguchi, S., Kobayashi, S., Saga, Y., 2003. Conserved role of nanos proteins in germ cell development. Science 301, 1239–1241.

Weisblat, D.A., Blair, S.S., 1984. Developmental indeterminacy in embryos of the leech *Helobdella triserialis*. Dev. Biol. 101, 326–335.

Weisblat, D.A., Huang, F.Z., 2001. An overview of glossiphoniid leech development. Can. J. Zool. 79, 218–232.

Weisblat, D.A., Zackson, S.L., Blair, S.S., Young, J.D., 1980. Cell lineage analysis by intracellular injection of fluorescent tracers. Science 209, 1538–1541.

Wreden, C., Verrotti, A.C., Schisa, J.A., Lieberfarb, M.E., Strickland, S., 1997. Nanos and pumilio establish embryonic polarity in *Drosophila* by promoting posterior deadenylation of *hunchback* mRNA. Development 124, 3015–3023.

Zackson, S.L., 1984. Cell lineage, cell–cell interaction, and segment formation in the ectoderm of a glossiphoniid leech embryo. Dev. Biol. 104, 143–160.

Zhang, S.O., Weisblat, D.A., 2005. Applications of mRNA injections for analyzing cell lineage and asymmetric cell divisions during segmentation in the leech *Helobdella robusta*. Development 132, 2103–2113.